horticulturae

MDPI

Article

Anther Ontogeny and Pollen Development in Southern Highbush Blueberry (*Vaccinium corymbosum* L.)

José María Recalde [1], Miguel Fernando Garavello [1], Paula Alayón Luaces [2] and Ana María González [2,3,*]

[1] INTA, Instituto Nacional de Tecnología Agropecuaria, Estación Experimental de Concordia, Concordia 3200, Argentina; joserecaldefca@gmail.com (J.M.R.); garavello.miguel@inta.gob.ar (M.F.G.)
[2] Facultad de Ciencias Agrarias, Universidad Nacional del Nordeste, Corrientes 3400, Argentina; palayonluaces@yahoo.com
[3] Instituto de Botánica del Nordeste, Consejo Nacional de Investigaciones Científicas y Técnicas—Universidad Nacional del Nordeste, Corrientes 3400, Argentina
* Correspondence: anagonzalez.ibone@gmail.com

Abstract

Southern highbush blueberry (SHB, *Vaccinium corymbosum*, Ericaceae) enables production in warm, low-chill regions, where breeding success depends on precisely timed pollinations. To support breeding in non-traditional environments, we characterized floral staging, anther wall ontogeny, tubule formation, and pollen development in two SHB cultivars ('Emerald', 'Snowchaser') grown in commercial orchards. Floral development was divided into seven stages: dormant buds (db), five successive floral-bud stages (botA–botE), and anthesis, based on bud size, corolla exposure and pigmentation, and anther/tubule coloration. Internal events were documented by light, confocal, and scanning electron microscopy. External cues reliably separated stages and tracked male-gametophyte phases: meiosis at botB; callose-encased tetrads at botC; permanent tetrahedral tetrads after callose dissolution at botD; bicellular tetrads from botE to anthesis, released intact via poricidal dehiscence. Anther-wall differentiation followed a consistent sequence and lacked a fibrous, lignified endothecium. We therefore propose a new Ericaceous pattern for blueberry anthers, defined by a transient non-lignified subepidermal stratum. Tubules originated apically as solid outgrowths, hollowed centrifugally to a beveled pore, developed a dorsal supportive zone, and mediated poricidal release of permanent tetrads. No qualitative cultivar differences were detected. The staging framework defines operational windows for pollination, emasculation, and pollen handling in low-chill systems.

Keywords: anther development; breeding resources; microsporogenesis; poricidal dehiscence; reproductive biology; *Vaccinium corymbosum*

check for updates

Academic Editor: Gunārs Lācis

Received: 1 October 2025
Revised: 19 October 2025
Accepted: 22 October 2025
Published: 24 October 2025

Citation: Recalde, J.M.; Garavello, M.F.; Alayón Luaces, P.; González, A.M. Anther Ontogeny and Pollen Development in Southern Highbush Blueberry (*Vaccinium corymbosum* L.). *Horticulturae* **2025**, *11*, 1278. https://doi.org/10.3390/horticulturae11111278

Copyright: © 2025 by the authors. Licensee MDPI, Basel, Switzerland. This article is an open access article distributed under the terms and conditions of the Creative Commons Attribution (CC BY) license (https://creativecommons.org/licenses/by/4.0/).

1. Introduction

Blueberries (*Vaccinium* L., Ericaceae) have expanded rapidly beyond their native range due to the development of Southern Highbush cultivars with reduced chilling requirements, enabling production in non-traditional environments [1–3]. Within *V. corymbosum* L., biotypes are distinguished by geographic origin, chilling requirements, and cold hardiness. Northern Highbush Blueberries (NHB) are native to regions with harsh winters and mild summers, while Southern Highbush Blueberries (SHB) were developed by hybridizing with *Vaccinium* species from the southern United States, resulting in cultivars with reduced cold tolerance [4]. This biotype has enabled large-scale blueberry cultivation in non-traditional regions worldwide [2]. SHB biotypes are now widely cultivated in warm

and subtropical regions, such as northeastern Argentina, where they have supported the expansion of large-scale blueberry production [5]. The success of these cultivars also depends on their reproductive efficiency, which in turn is strongly influenced by floral structure and pollination mechanisms [6].

Vaccinium flowers share a suite of characters associated with buzz-pollination: pendulous, epigynous corollas, introrse stamens bearing elongated apical tubules, poricidal dehiscence, and permanent tetrahedral tetrads released at anthesis [7,8]. These floral traits are functionally relevant to reproductive success and breeding efficiency in *V. corymbosum*. Genetic improvement programs for *V. corymbosum* are primarily based on traditional methods, generating progeny from open-pollinated seed or controlled crosses, followed by the selection of individuals with desirable traits [9–11].

In angiosperms, understanding anther and pollen development is essential to elucidate the reproductive mechanisms that determine fruit set and seed quality, and this is equally valid for blueberries (*Vaccinium* spp.). These processes are particularly sensitive to environmental stress, which can affect male gametogenesis and, consequently, fertilization efficiency [12–14]. Previous studies have linked pollen viability and inter-cultivar compatibility with key production parameters such as fruit set, seed number, and berry size [15,16].

Detailed developmental studies on anther and pollen formation remain scarce, and no recent analyses have addressed these processes in SHB cultivars. Most embryological and cytological research on *Vaccinium corymbosum* was conducted several decades ago and focused mainly on NHB cultivars such as 'Bluecrop' and 'Croatan', providing only limited information on anther wall-layer differentiation in relation to microsporogenesis and pollen maturation [17,18]. To date, no comparable analyses have been performed for SHB cultivars, including 'Emerald' and 'Snowchaser', the two varieties examined in this study, despite their increasing relevance for warm-climate blueberry production systems in regions such as northeastern Argentina and other subtropical areas worldwide.

Considering the intrinsic variability of stamen structure within Ericaceae and the central role of male reproductive biology in breeding, a focused analysis of anther development and pollen formation in *V. corymbosum* is warranted, as current knowledge remains limited and constrains both basic understanding and applied improvement in southern highbush blueberries. Therefore, this study aimed to (i) establish a high-resolution floral staging scale for SHB and validate it against male gametophyte development; (ii) characterize anther wall and tubule anatomy and ontogeny; (iii) integrate morphology, anatomy, and cytology into a practical crosswalk that maps our stages onto Michigan State University (MSU) [19] and BBCH phenology scales [20].

2. Materials and Methods

2.1. Study Sites and Environmental Conditions

Sampling was conducted during the 2022 and 2023 growing seasons in northeastern Argentina (NEA) in Concordia (Entre Ríos) and Bella Vista (Corrientes). In Concordia, the climate is humid subtropical, with an average annual temperature of 19 °C and mean rainfall of 1300 mm. Soils are deep and sandy, with low organic matter and slightly acidic pH (5.0–5.5) [21,22]. On the other hand, in Bella Vista, the climate is also humid subtropical, with an average annual temperature of 20.7 °C and rainfall of 1400 mm, showing marked seasonal variation. Soils are sandy-loam with low fertility and weak water retention [23]. Plants were grown on raised beds covered with black plastic mulch, with frost control by overhead irrigation, and managed according to standard commercial practices for blueberry production in this northeastern Argentine region.

2.2. Plant Material

Flowers were collected from field-grown plants of two *V. corymbosum* SHB cultivars: 'Emerald' (12-year-old plants) and 'Snowchaser' (8-year-old plants), widely cultivated in the region for their agronomic performance and low-chill adaptation [5]. Voucher specimens were deposited in the IBONE herbarium "Carmen L. Cristóbal" (CTES) with full locality data and collection numbers.

2.3. Floral Bud and Flower Staging

Floral buds, and flowers at anthesis were classified individually using external cues (bud length and diameter, degree of corolla exposure and pigmentation, and anther/tubule coloration). Stages included dormant buds (db), five floral-bud stages (botA–botE), and anthesis (ant). Reference length/diameter values are presented in Table 1, and representative buds are shown in Figure 1 (see Results Section for a concise descriptive summary). For agronomic comparability, our staging was anchored to the Michigan State University (MSU) [19], and BBCH phenological descriptors [20] while providing finer resolution to map external bud traits onto internal cytological events. Stage assignment was made at collection from external morphology and subsequently validated cytologically on a subset of samples (see Microscopy sections below).

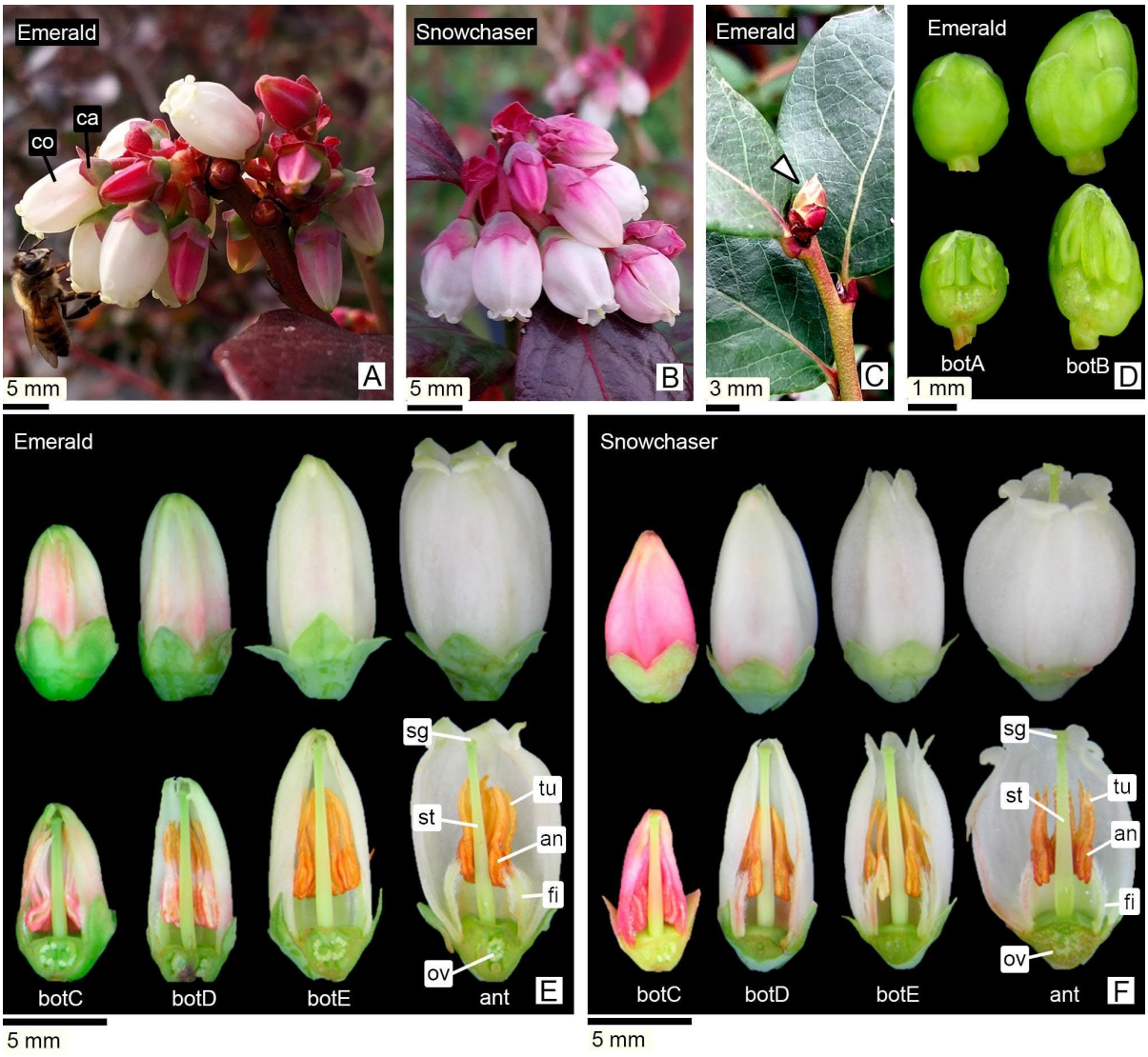


Figure 1. Inflorescences, floral buds and flowers. (**A**,**B**) Racemes; (**C**) Dormant bud (indicated by arrow). (**D**) Surface view and LS of early-stage buds (botA and botB). (**E**,**F**) Surface view and LS: Developmental

sequence of floral buds (botC, botD, botE) and flower at anthesis (ant). Reproductive organs are indicated only in flowers at anthesis. Abbreviations: an, anther; ca, calyx; co, corolla; fi, filament; ov, ovary; sg, stigma; st, style; tu, tubule. Image types: (**A**–**C**) Field photographs; (**D**–**F**) SM.

Table 1. Classification of floral stages for *V. corymbosum* Southern Highbush Blueberries.

Stage	Larger Diameter (mm)	Length (mm)	Perianth Color and Characteristics	Anther Color		Tubules Color	
				'Emerald'	'Snowchaser'	'Emerald'	'Snowchaser'
db	<1	<1.2	Not visible. Flower bud covered by bracts of dormant reproductive bud.	Not externally visible		Not externally visible	
botA	1–1.5	1.2–1.6	Green calyx, hidden corolla.	Green		Green	
botB	1.5–2	1.6–3	Green calyx, hidden corolla.	Green		Green	
botC	2–2.5	3–8	The pink corolla begins to emerge.	Soft pink	Deep pink	Whitish	Pink
botD	2.5–4.5	8–10.5	Pink corolla with white shades.	Whitish	Ochre	Orange–ochre	
botE	4.5–5	10.5–11.5	Corolla white, petals apex begin to separate.	Orange–ochre		Orange–ochre	
ant	5–7	10.5–11.5	White corolla, flower at anthesis.	Orange–ochre		Orange–ochre	

External staging of floral buds (db, botA–botE, ant) and diagnostic cues used at collection. References: ant: flower at anthesis; botA–E: floral buds A to E; db: dormant bud.

2.4. Sample Collection and Preparation

Healthy and vigorous plants located away from the edges of the orchards were selected for sampling to ensure representative material. For each developmental stage, approximately 30 floral buds and flowers were collected per cultivar to ensure adequate sampling. From these, 3–5 were selected and processed for anatomical and cytological analyses based on the previously classified buds and flowers. The prepared samples allowed the identification of representative developmental features at each floral stage. Observations were performed on fresh and FAA-fixed floral material (FAA: 70% ethanol: formalin 37–40%: glacial acetic acid = 90:5:5, *v*/*v*, Cicarelli, Argentina) for morphological and anatomical analyses. Selected samples were examined through microscopic techniques, as described below.

2.5. Microscopy Analyses

2.5.1. Stereomicroscopy (SM)

Floral structures were examined using a Leica MZ6 stereomicroscope equipped with a digital imaging system (Flexacam C1, both of Leica Microsystems, Wetzlar, Germany). Morphometric measurements were obtained using Fiji software version 2.9.0; [24], following the methodology described by Gonzalez [25].

2.5.2. Light Microscopy (LM)

Samples were dehydrated in a graded ethanol series with clearing agents [26], embedded in paraffin [27], and sectioned at 12.5 µm thickness using a MICROM HM300 rotary microtome (Thermo Fisher Scientific, Walldorf, Germany). Transverse (TS) and longitudinal sections (LS) were stained with safranin (Sigma-Aldrich, Darmstadt, Germany)-astra blue (Biopack, Argentina) [28] and observed under a Leica DM LB2 light microscope with a Leica ICC50 HD camera (Leica Microsystems). For floral vascularization analysis and to evaluate the presence of a fibrous/mechanical endothecium, samples were cleared in 10% NaOH (Cicarelli, Argentina) for 8 h at 60 °C, thoroughly rinsing and stained with either toluidine blue (Sigma-Aldrich, Darmstadt, Germany) or safranin [29].

2.5.3. Confocal Laser Scanning Microscopy (CLSM)

Selected paraffin-embedded sections were deparaffinized and stained with 0.3% acridine orange Sigma-Aldrich, Darmstadt, Germany; [30]. Observations were conducted using a Stellaris 8 White Light Laser inverted confocal microscope (Leica Microsystems),

equipped with HC PL APO 10× dry (NA 0.4) and 63× oil immersion (NA 1.4) objectives. Excitation and emission wavelengths were set as follows: blue (488/498–530 nm), green (503/508–633 nm), and red (647/653 nm). Images were acquired and processed using LAS Navigator software (module of Leica Application Suite X, version 5.3.0, Leica Microsystems), which was also employed to stitch multiple fields into composite images.

2.5.4. Scanning Electron Microscopy (SEM)

FAA-fixed material was dehydrated in an ascending acetone series, critical-point dried, sputter-coated with gold, and examined in a JEOL LV 5800 (JEOL, Ltd., Tokyo, Japan) at 20 kV (Electron Microscopy Service of the Universidad Nacional del Nordeste).

3. Results

3.1. Floral Staging and General Flower Morphology

3.1.1. Inflorescence and Flower Overview

Plants of both SHB cultivars ('Emerald' and 'Snowchaser') bore short axillary racemes with pendulous, epigynous, actinomorphic flowers (Figure 1A,B). Corollas were urceolate–campanulate, white to pale cream, with five lobes; calyces were persistent. Flowers had ten introrse stamens bearing elongated apical tubules, and a single style arising from an inferior ovary (Figure 1C–F). These external features were consistent across sites and years, and no cultivar-specific differences were evident at this level of description.

3.1.2. Floral Staging

External bud traits scaled predictably with development and allowed us to distinguish dormant buds (db), five floral-bud stages (botA-botE), and anthesis (ant). Staging was applied consistently in both SHB cultivars, 'Emerald' and 'Snowchaser'. Table 1 summarizes the operational size thresholds and diagnostic external cues used for stage assignment, and Figure 1 shows representative buds.

Briefly, db comprised closed dormant buds with no visible corolla (Figure 1C); botA remained closed and green (Figure 1D); botB showed the first corolla ridge beneath the calyx (Figure 1D); botC displayed emerging, pale pink corolla and green anthers (Figure 1E,F); botD had one-third to two-thirds corolla expansion with the color transitions from pink to white, progressing from the apex toward the base and discernible tubule tips (Figure 1E,F); botE reached two-thirds or more of final corolla length with pigmented anthers/tubules while the perianth remained closed (Figure 1E,F). At anthesis (ant), the petal lobes separate, the corolla is entirely white in both cultivars, with poricidal pollen release and the stigma is positioned approximately at the level of the petal tips (Figure 1E,F). Although size ranges partially overlapped between adjacent stages, the combination of corolla exposure/pigmentation and anther/tubule coloration provided consistent discrimination at collection (Table 1).

Within the limits of our sampling, no marked cultivar-specific differences were evident in external cues or thresholds; results are therefore presented jointly unless noted otherwise. This staging was applied consistently throughout the study to facilitate the anatomical and ontogenetic analysis of anther and pollen development.

3.2. Androecium Ontogeny: Morphological and Anatomical Insights

In flowers at anthesis, the androecium consists of ten stamens (occasionally 9–11), free and introrse, each formed by a filament and a dorsifixed, versatile, dithecous anther that extends apically into two hollow tubules (Figure 2A–C). From botC to botD, anthers and tubules are white to pinkish, turning intense orange–ochre at anthesis (Figure 1E,F). The tubules, oriented toward the style from early stages through anthesis (Figure 2A–C), develop a beveled apical pore in the more advanced stages (botC–ant; Figure 2D–F). Both

thecae and tubules acquire a slight S-shaped curvature, positioning the pollen sacs and tubule openings toward the style while remaining below the stigma level (Figure 2A–C).

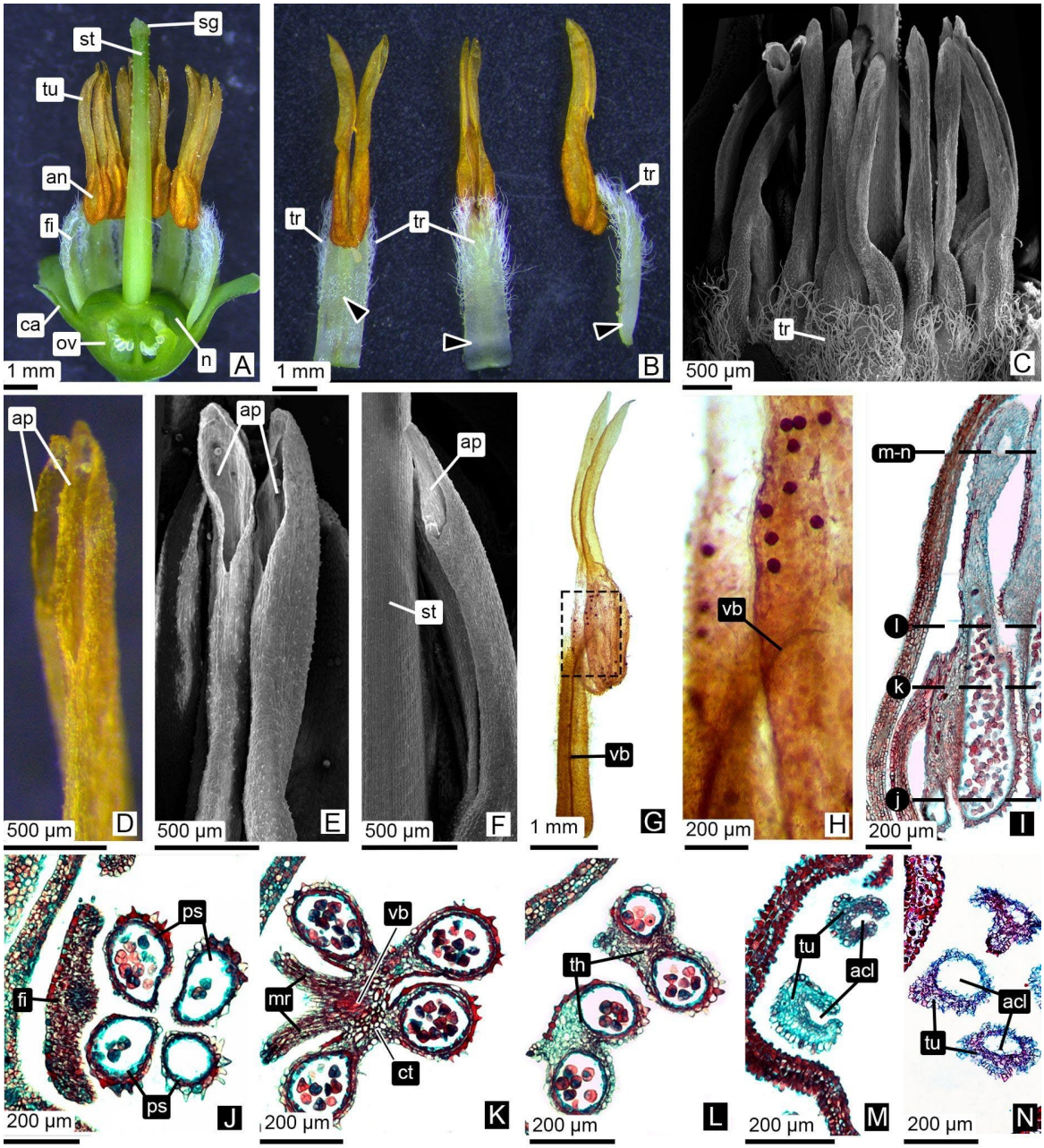


Figure 2. Stamens: overview, vascularization, and anatomy. (**A**) LS of flower at anthesis: overall arrangement of stamens and tubules relative to the style (corolla removed). (**B**) Stamens at anthesis (ventral left, dorsal center, lateral right); arrows: glabrous filament region. (**C**) Androecium at anthesis, showing the indumentum of the staminal filaments. (**D**–**F**) Detail of oblique apical pores in the tubules (anthesis). (**G**) Lateral view of a cleared stamen showing its vascular pattern. (**H**) Close-up showing the vascular bundle entering the dorsal side of the anther (region indicated in (**G**)). (**I**) LS of a stamen of a botC, showing the pore at the apex of the tubules and indicating the levels of TS in (**J**–**N**). (**J**) Filament and anther base, showing four pollen sacs. (**K**) Vascular bundle concentrated in a circular zone within the connective tissue. (**L**) Apical region of the pollen sacs. (**M**,**N**) Apical zone of the tubules where internal parenchyma degradation begins. Abbreviations: acl, apical cleft; an, anther; ap, apical pore; ca, calyx; ct, connective tissue; fi, filament; mr, multicellular ridges; n, nectary; ov, ovary; ps, pollen sac; sg, stigma; st, style; th, theca; tr, trichomes; tu, tubules; vb, vascular bundle. Image type: (**A**,**B**,**D**,**G**,**H**) SM; (**C**,**E**,**F**) SEM, (**I**–**N**) LM. Cultivars: (**A**,**B**,**D**–**M**) ‘Emerald’; (**C**,**N**) ‘Snowchaser’.

A single vascular bundle runs the filament and enters the connective tissue (Figure 2G), where it briefly extends into the base of the thecae before terminating (Figure 2H). The upper portion of the thecae, as well as the tubules, lacks vascular tissue (Figure 2G).

The staminal filament is dorsally inserted on the thecae (Figure 2G,I) and is green and laterally flattened (Figure 2A,B). The filament is glabrous at its base and along the entire adaxial surface, while the middle and upper portions of the abaxial surface and margins are densely covered with white, simple, non-secretory trichomes. (Figure 2B,C).

Transverse sections reveal that the four pollen sacs remain independent at the base of the thecae (Figure 2J). The connective tissue is formed by parenchymatous cells surrounding the vascular bundle and extending dorsally within the anther (Figure 2K). A small region of connective tissue is present only at the junction with the filament (Figure 2K), above which the thecae are completely separate (Figure 2L). In this region, the filament margins expand slightly to form two low, multicellular ridges that do not exceed the height of the pollen sacs (Figure 2K,L). Each theca continues apically into a single hollow tubule, resulting in four pollen sacs per stamen but only two apical tubules through which pollen is released (Figure 2L–N).

3.2.1. Anther Wall Ontogeny

In dormant buds, key steps of anther-wall differentiation are already initiated. In the transverse section the anther is quadrangular to rectangular, with a single epidermal layer enclosing an archesporial mass and a central connective (Figure 3A). Pollen sacs begin to form at the four corners. Periclinal divisions of the archesporial cells generate a primary parietal layer outward and sporogenous tissue inward (Figure 3B). Further divisions of the parietal layer produce an outer and an inner secondary parietal layer (Figure 3C,D). The outer secondary parietal layer yields two middle layers, whereas the inner secondary parietal layer gives rise to an additional middle layer and the tapetum (Figure 3E–H). These divisions are not uniform around the sac, being more frequent on the side adjacent to the connective (Figure 3H).

In botA the anther wall consists of the epidermis, two to three middle layers, and the tapetum (Figure 3F–H). The epidermis bears a thin cuticle and lacks stomata (Figure 3H). During meiosis (botB), tapetal cells enlarge, become binucleate, and begin to lose their compact arrangement (Figure 3I). At the tetrad stage (botC), the tapetum is reduced and the middle layers begin to collapse, while the epidermis above the pollen sacs develops papillate thickenings (Figure 3J,K). This papillate condition is confined to epidermal cells overlying the sacs.

In buds approaching anthesis (botD–E), the tapetum is completely degraded or persists as thin remnants, and middle layers are largely collapsed, often reduced to one residual stratum (Figure 3L). In mature anthers, the wall is composed almost exclusively of the epidermis (Figure 3M,N). Papillae remain restricted to the epidermis over the pollen sacs, whereas the epidermis above the connective tissue is rough and non-papillate (Figure 3O,P). Critically, no endothecial-type fibrous thickenings were detected in either cultivar with any technique: neither in safranin–astra blue-stained sections nor in NaOH-cleared anthers examined under light microscopy. This corroborates the absence of a functional mechanical endothecium.

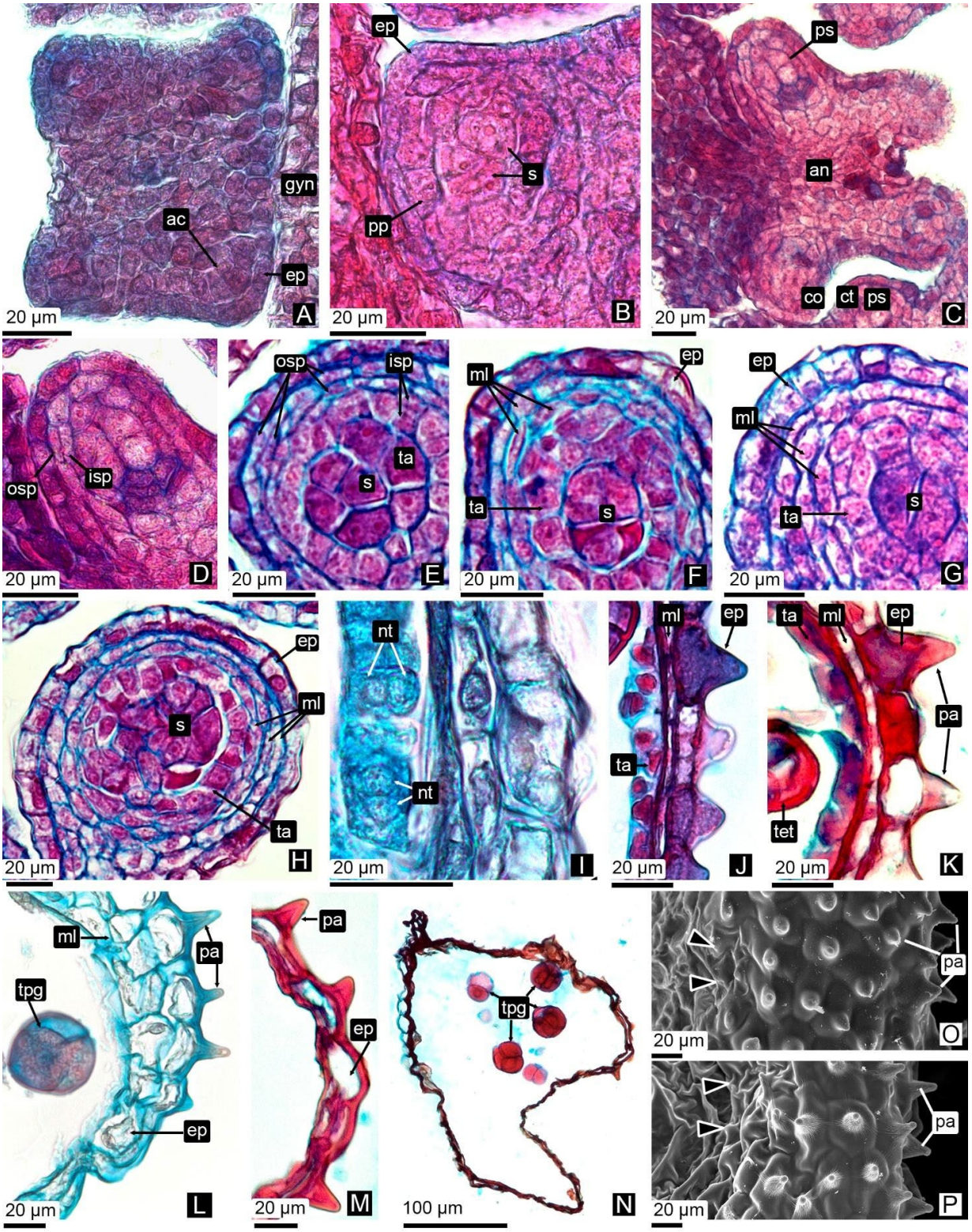


Figure 3. Anther wall ontogeny. (**A**) Anther primordium from db; (**B**) Pollen sac with archesporial cells of young anthers from db; (**C**) Tetralobed anther from db; (**D**) Close-up of a pollen sac from the anther shown in (**C**); (**E**) Pollen sac showing the inner and outer secondary parietal layer undergoing periclinal divisions to form the anther wall layers; (**F**–**H**) Pollen sac from a botA and detail of its constituent layers; (**I**) Binucleate tapetal cells of a botB; (**J**,**K**) Pollen sacs from a botC; (**L**) Pollen sac of a botE; (**M**,**N**) Pollen sacs at anthesis; (**O**,**P**) Surface view of the anther showing the connective region without papillae (indicated by arrows) and a papillose epidermis over the pollen sacs. Abbreviations:

ac, archesporial cells; an, anther; co, corolla; ct, connective tissue; ep, epidermis; gyn, gynoecium; isp, inner secondary parietal layer; ml, middle layers; nt, tapetal cell nucleus; osp, outer secondary parietal layer; pa, papilla; pp, primary parietal layer; ps, pollen sac; s, sporogenous cell; ta, tapetum; tet, tetrad of microspores; tpg, tetrad of pollen grains; vb, vascular bundle. Image types: (**A**–**N**) LM; (**O**–**P**) SEM. Cultivar: (**E**–**G**,**K**,**M**,**O**) 'Emerald'; (**A**–**D**,**H**–**J**,**L**,**N**,**P**) 'Snowchaser'.

3.2.2. Pollen Grain Formation

In dormant buds (db), the sporogenous tissue forms a compact mass of uninucleate cells (Figure 4A). Successive mitotic divisions generate microspore mother cells (MMCs), which enlarge during interphase and develop expanded nuclei with conspicuous nucleoli and early chromatin condensation (Figure 4B).

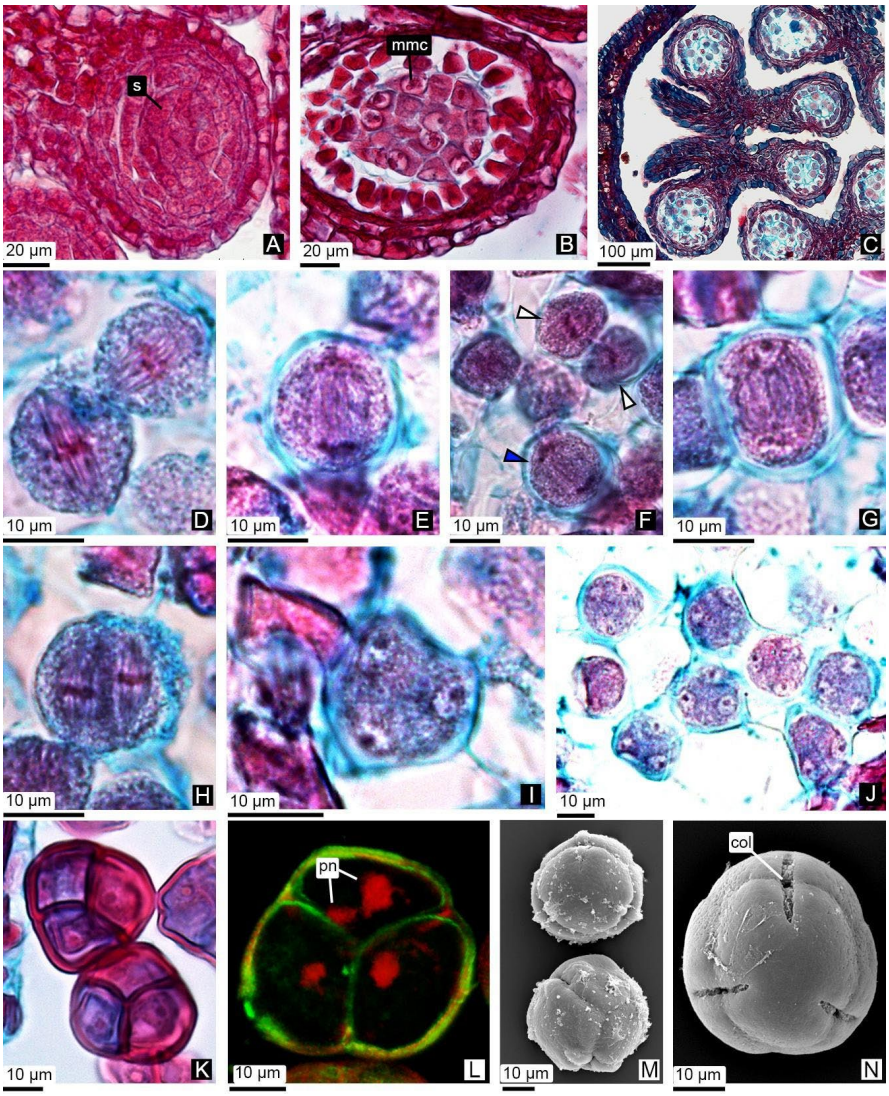


Figure 4. Microsporogenesis. (**A**) Pollen sac of a dormant bud (db); (**B**) Pollen sac of a botA; (**C**) Anther of a botB at the meiosis stage; (**D**–**J**) Reproductive cells of a botB undergoing meiosis: (**D**) Metaphase I; (**E**) Anaphase I; (**F**) Cells at metaphase I (white arrow) and anaphase I (blue arrow) within the same pollen sac; (**G**) Telophase I; (**H**) Metaphase II; (**I**) Telophase II; (**J**) Cells at telophase II within the same pollen sac; (**K**) Tetrads of microspores in a botC; (**L**) Tetrad showing one binucleate pollen grain; (**M**,**N**) Tetrads of pollen grains at anthesis. Abbreviations: col, colporus; mmc, microspore mother cell; pn, pollen nuclei; s, sporogenous cell; Image types: (**A**–**K**) LM, TS; (**L**) CLSM, TS; (**M**,**N**) SEM. Cultivar: (**N**) 'Emerald'; (**A**–**M**) 'Snowchaser'.

Meiosis occurs in anthers at the botB stage (Figure 4C). Both meiotic divisions proceed normally (Figure 4D–K), and different meiotic phases may coexist within the same sac (Figure 4F). Cytokinesis is simultaneous, yielding tetrahedral tetrads with the four nuclei positioned at the vertices (Figure 4I,J). Tetrads first appear at botC, with the tapetum and middle layers still present in the anther wall (Figure 4K).

The microspores remain attached, forming permanent tetrahedral tetrads. Each microspore undergoes a mitotic division, producing bicellular pollen grains (Figure 4L). Mature pollen grains are released in tetrads. Each pollen grain is tricolporate, with colpi aligned so that two adjacent grains appear to share a single furrow, and the exine is rugulate without prominent sculptural elements (Figure 4M,N).

3.2.3. Tubule Ontogeny and Pollen Tetrad Release

Early development: From botA, tubule primordia appear at the apex of each theca as solid outgrowths of parenchymatous cells lacking intercellular spaces or vascular supply (Figure 5A,B). The epidermis is single-layered and lacks stomata. At this stage (floral-bud stage B), each theca still encloses two independent pollen sacs that are not yet connected to the developing tubule, and meiosis is underway in the microspore mother cells (MMCs).

Cavity formation in the tubule: By floral-bud stage botB, the tubule's central parenchyma begins to degenerate centrifugally from the apex downward, producing first a shallow apical cleft (Figure 5D–F) that develops into the beveled apical pore. The pollen sacs remain separated (Figure 5G). At this stage, the two pollen sacs in each theca remain separate in their apical portion (adjacent to the developing tubule, Figure 5G).

Maturation: In botE and anthesis, the tubules are fully hollow, sometimes retaining a few layers of subepidermal parenchyma (Figure 5H–J), and displaying a dorsal thickening on the outer side of their middle portion (Figure 5K). At the apical portion of each theca, the septum separating the two pollen sacs disintegrates, generating a single cavity that connects directly with the tubule (Figure 5L–O). Basally and near the connective, the sacs remain distinct (Figure 5P,Q). A dorsal supporting tissue develops and extends toward the beveled opening (Figures 5K–N and 6A–C); its parenchymatous cells exhibit slight wall thickening with simple pits (Figure 6E). At the apex, the cells lining the pore bear surface papillae (Figure 6B–F).

Pollen release: Permanent pollen tetrads move from the sacs into the tubules and are expelled through the beveled apical pores (Figures 5H–Q and 6B,C).

No qualitative differences were detected between 'Emerald' and 'Snowchaser' in the characteristics or developmental patterns of the pollen, anther wall, or tubule. Morphological variation between cultivars was restricted to subtle color differences in anthers and tubules during intermediate floral stages (botC–botD), as shown in Table 1, where 'Emerald' exhibited lighter tones and 'Snowchaser' slightly deeper pigmentation. The anatomical and cytological features summarized in Table 2 were fully consistent across both genotypes. Equivalent stages of 'Emerald' and 'Snowchaser' are illustrated in paired panels (e.g., Figures 2E,F, 3G,H,J,K, 4M,N, 5Q,R and 6), confirming the uniformity of structural and developmental traits; therefore, observations were pooled.

Table 2 synthesizes floral development by integrating external staging (morphology) with anatomical–ontogenetic (anther wall and tubule ontogeny) and cytological (microsporogenesis/microgametogenesis) results. It also maps our stages onto the phenological descriptors used for *V. corymbosum* by Michigan State University and the BBCH system, focusing on reproductive phases. This crosswalk indicates the phenological windows in which each floral-bud size in our scale is most frequently observed, spanning BBCH stage 00 (dormancy) and macrostages 5–6.

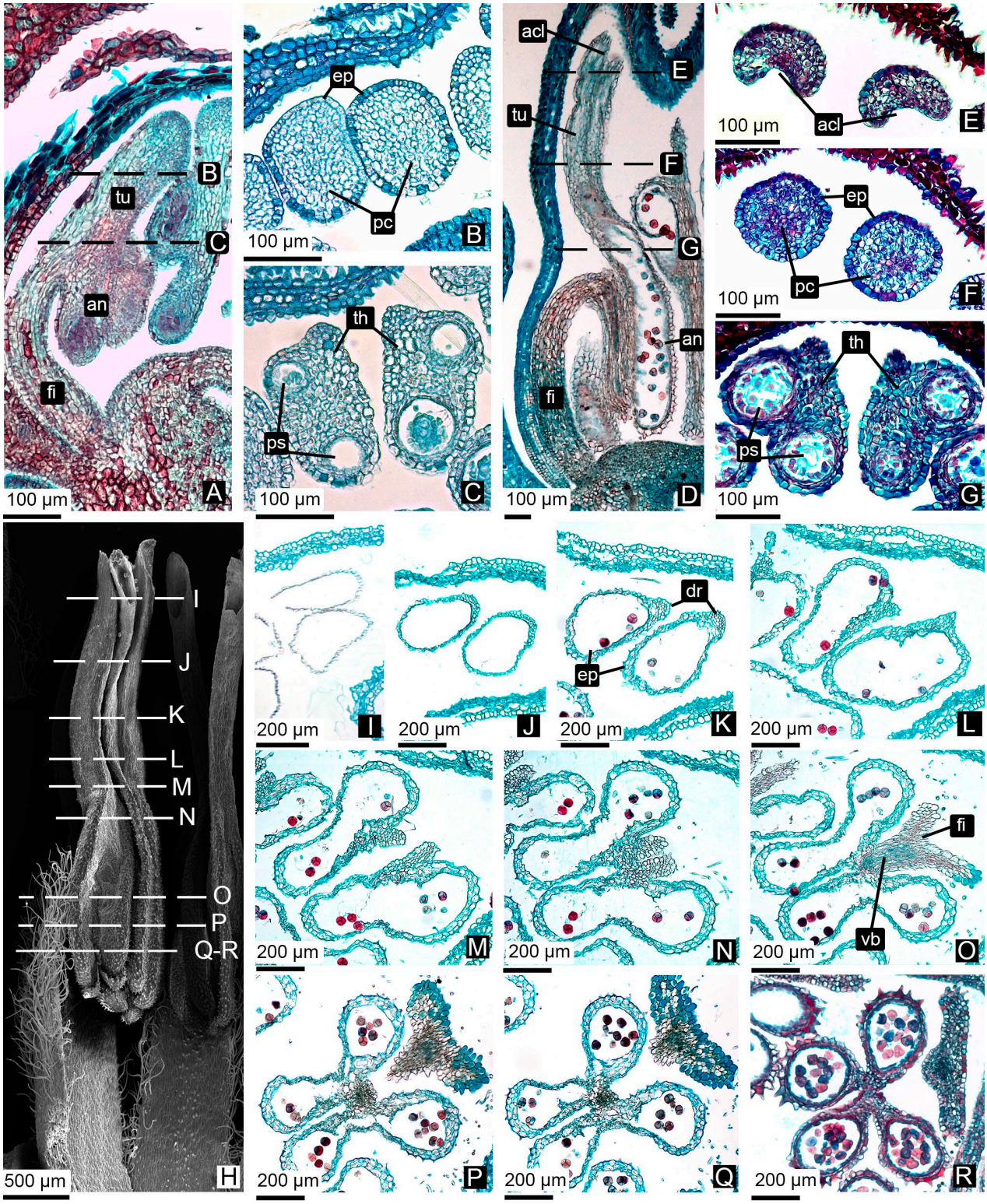


Figure 5. Ontogeny of anther tubules. (**A**) LS of a stamen from botA, indicating the levels of the TS in (**B**,**C**); (**B**) Solid tubules; (**C**) Separation of thecae; (**D**) LS of a stamen from botB, indicating the levels of TS in (**E**–**G**); (**E**) Apex of tubules; (**F**) Solid tubules; (**G**) Thecae separation; (**H**) General view of a stamen at anthesis, showing the levels of TS in (**I**–**R**); (**I**) Tubule apex; (**J**) Hollow tubules; (**K**,**L**) Hollow tubules with dorsal reinforcement; (**M**,**N**) Anther views; (**O**) Filament insertion on the dorsal side of the anther; (**P**–**R**) Separated anther and filament. Abbreviations: acl, apical cleft; an, anther; dr, dorsal reinforcement; ep, epidermis; fi, filament; pc, parenchymatous cells; ps, pollen sac; th, theca; tu, tubules; vb: vascular bundle. Image types: (**A**–**G**,**I**–**Q**) LM; (**H**) SEM. Cultivar: (**A**,**R**) 'Emerald'; (**B**–**Q**) 'Snowchaser'.

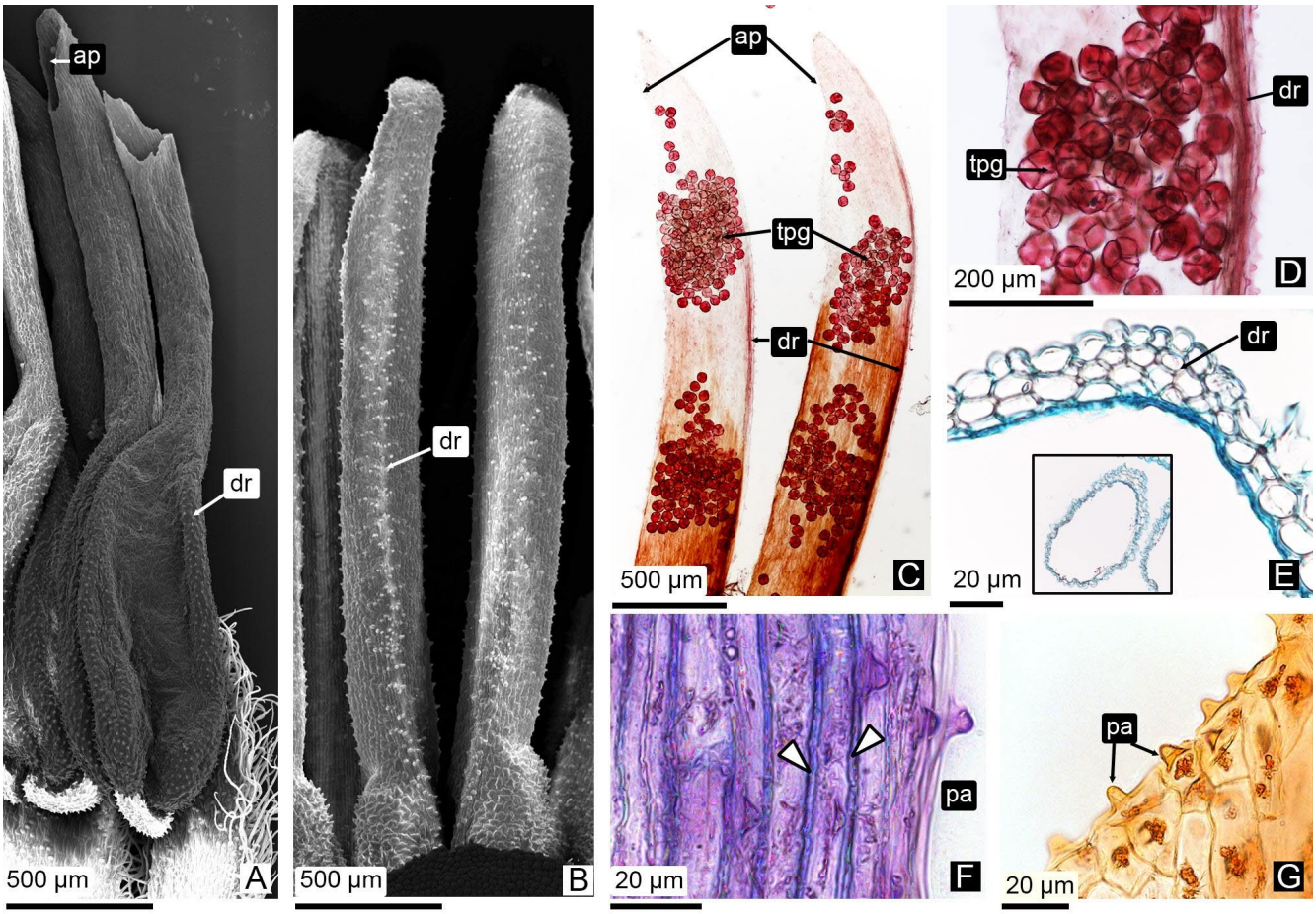


Figure 6. Dorsal reinforcement of anther tubules at anthesis. (**A**) Lateral view of stamens; (**B**) Dorsal view of anther tubules; (**C**) Cleared tubules showing beveled apical pores (ap) and poricidal release of permanent pollen tetrads (tpg); dorsal reinforcement with supportive tissue (dr); (**D**) Detail of an anther tubule; (**E**) Cross-section of a tubule and detail of dorsal reinforcement; (**F**) Outer wall of an anther tubule (arrows indicate the simple pits); (**G**) Papillose surface at the apex of an anther tubule. Abbreviations: ap, apical pore; dr, dorsal reinforcement; pa, papilla; tpg, tetrad of pollen grains. Image types: (**A**,**B**) SEM; (**C**,**D**,**F**,**G**) SM; (**E**) LM. Cultivar: (**A**,**E**) 'Snowchaser'; (**B**–**D**,**F**,**G**) 'Emerald'.

Table 2. Floral bud and anthesis stages of Southern Highbush Blueberry (*V. corymbosum*), integrating pollen and anther development. Stages are aligned with the MSU and BBCH phenological scales. Floral stages (db, botA–E, ant) are defined in Table 1.

Floral Stages (This Paper)	MSU	BBCH	Pollen Development Stage	Main Morphological Event	Anther Tissues	Tubule
db	Dormant or tight bud.	00 Dormancy. Flower buds are tightly closed.	Archesporial cells.	Anthers initially quadrangular, later tetralobed.	(1°) Epidermis, archesporial cells; (2°) Epidermis, primary parietal layer, sporogenous tissue; (3°) Epidermis, layer forming.	Developing.
botA	Bud swells.	51 Inflorescence buds swelling. Bud scales elongated, with light colored margins.	Sporogenous tissue.	Compact MMCs observed in pollen sacs, with expanded nuclei and high chromatin content.	Epidermis, middle layers, tapetum, sporogenous tissue/MMCs, connective tissue, vascular bundle.	Solid. Epidermis encloses a mass of parenchymatous cells.

Table 2. *Cont.*

Floral Stages (This Paper)	MSU	BBCH	Pollen Development Stage	Main Morphological Event	Anther Tissues	Tubule
botB	Bud break or bud burst.	53 Inflorescence bud burst. Bud scales separated, lightened bud areas are visible.	Meiosis.	Locules expand, and internal cells become loosely arranged. Microspore mother cells undergo meiosis. Binucleate tapetum.	Epidermis, middle layers, tapetum, MMCs, connective tissue, vascular bundle.	Onset of central parenchyma degradation. Formation of apical slit.
botC	Tight cluster.	55 Green bud stage. First flower buds visible, tight flower clusters, flower buds are still closed.	Tetrads of microspores	Simultaneous cytokinesis in tetrads. Tetrads are surrounded by callose.	Epidermis, middle layers, tapetum, tetrads, connective tissue, vascular bundle.	Hollow in the central region. Epidermis with adjacent layers of parenchymatic cells.
botD	Early pink bud	57 Early pink bud stage. Flower buds are separating, still closed and pink, pedicels are elongating.	Callose dissolves, releasing tetrads.	Fusion of pollen sacs within each theca occurs only at the apex, continuing into a tubule.	Epidermis, tetrads, connective tissue, vascular bundle.	Hollow. Tubule wall consisting of one or two cell layers.
botE	Late pink bud.	59 Late pink bud. All flower buds are fully developed but still closed, the expanded petals are white now.	Tetrads of bicellular pollen grains.	Anthers contain tetrads of bicellular pollen grains.	Epidermis, tetrads, connective tissue, vascular bundle.	Hollow. Tubule wall consisting of one or two cell layers.
ant	Full bloom	65 Full flowering. At least 50% of the flowers are open.	Anther dehiscence, tetrad release.	The permanent tetrads are released through the tubules. The anther remains composed of epidermis.	Epidermis, tetrads, connective tissue, vascular bundle.	Hollow. Tubule wall composed only of epidermis.

4. Discussion

4.1. Floral Morphology and Anther Development

This study characterizes the floral structure of *V. corymbosum* SHB, reaffirming its alignment with the diagnostic traits of the Ericaceae family, including urceolate, sympetalous corolla and introrse stamens with poricidal dehiscence, features commonly reported in the family [8,31]. The actinomorphic and hermaphroditic conditions observed in both cultivars align with descriptions for several *Vaccinium* species [32,33]. Variability in the number of floral organs per whorl has been described in *Vaccinium*, with pentamerous and hexamerous flowers reported across species [34,35]. However, this study found no such variation between the two cultivars analyzed, confirming structural consistency within *V. corymbosum* SHB.

Beyond the general floral traits, particular attention was given to the internal architecture of the androecium in *V. corymbosum* SHB, as observed in the cultivars 'Emerald' and 'Snowchaser', which conforms to the patterns described for Ericaceae and *Vaccinium* species, including the number and arrangement of stamens, dorsifixed anthers with apical tubules, and the insertion of the vascular bundle into the connective tissue [34,35]. In the subfamilies Arbutoideae Nied., Ericoideae Link, Rhododendroideae Endl., and Vaccinioideae Arn., the filament attaches to the dorsal side of the anther, and the vascular bundle entering the connective curves downward toward the base of the anther [36]. As observed by Palser [34] in *V. corymbosum* (cultivar not specified), the vascular tissue extends into the anther beyond this curvature. In the present study, the vascular bundle followed a similar trajectory but did not reach the basal region of the anther in either 'Emerald' or 'Snowchaser'.

In addition to internal anatomical features, the surface characteristics of the filament were also examined. Unicellular trichomes have been described on the filaments of *V. corymbosum* [34], while both unicellular and multicellular types have been reported in *V. albicans* Sleumer [7], *V. vitis-idaea* L., and *V. myrtilloides* Michx. [35]. In the latter two species, trichomes are restricted to the lateral sides of the filament. In contrast, both 'Emerald' and 'Snowchaser' exhibited abundant trichomes not only on the lateral surfaces but also on the abaxial side of the filament.

Further examination of the anther surface revealed distinct epidermal patterns, particularly in the thecae and connective regions. In both 'Emerald' and 'Snowchaser,' the epidermis over the thecae exhibited a papillose surface, while the connective region remained smooth. This pattern is consistent with prior reports for *V. vitis-idaea* and *V. myrtilloides* [35], as well as for *V. nummularia* Hook., *V. serratum* Sleumer, and *V. retusum* (Griff.) Hook. [33]. Similar distribution of papillae has also been observed in other Ericaceae, such as *Arbutus unedo* L. and *Arctostaphylos manzanita* Parry, where papillae were restricted to the ventral surface and flanks of the anther lobes [31]. The absence of papillae on the connective appears to be a conserved trait within the family and is reaffirmed in the present study.

Taken as a whole, these observations provide a comprehensive morphological framework for the floral and androecial structures of *V. corymbosum* SHB, supporting its placement within Ericaceae and informing subsequent analyses of reproductive development.

4.1.1. Anther Wall Ontogeny

To further understand the reproductive anatomy of *V. corymbosum* SHB, the ontogeny of the anther wall was examined in detail. In Ericaceae, a common anther wall structure was observed, comprising an epidermis, a hypodermal "endothecial" layer (despite lacking the characteristic fibrous thickenings), one or more middle layers, and a secretory-type tapetum [7]. As development progresses, these layers gradually degenerate, and by the time of dehiscence, only the epidermis typically remains [7]. In several *Vaccinium* species (*V. nummularia*, *V. serratum*, *V. retusum*, *V. albicans*, *V. stamineum* L., *V. vitis-idaea*, and *V. myrtilloides*) this general organization has been consistently reported [7,33,35]. In *V. corymbosum* NHB, previous studies in the cultivars 'Bluecrop' and 'Croatan' described aspects of tapetum development and microsporogenesis, but did not provide direct observations or detailed accounts of anther wall layer differentiation or ontogeny [17,18].

Apical dehiscence in Ericaceae has been associated with the absence of a differentiated endothecium [7] and with hygroscopic movements of the epidermal cells [20]. In a broad anatomical sense, the endothecium refers to the anther wall layer whose cells develop fibrous thickenings [37]. However, multiple studies have reported the absence of this layer in *Vaccinium* species, including *V. nummularia*, *V. serratum*, *V. retusum*, *V. albicans*, *V. stamineum*, *V. vitis-idaea*, and *V. myrtilloides* [7,31,33,35], supporting the view that *Vaccinium* lacks a true mechanical layer in the anther wall.

Consistent with these reports, our observations (based on material from the cultivars 'Emerald' and 'Snowchaser') revealed that in the young anther, *V. corymbosum* SHB exhibits a typical organization consisting of an epidermis, one to several middle layers, and a secretory-type tapetum. As development progresses, these layers gradually degenerate, and the mature anther wall is reduced to a single epidermal layer lacking endothecial thickenings (Figure 7), consistent with previous reports for other *Vaccinium* species and members of Ericaceae. These findings support the hypothesis that apical dehiscence in *V. corymbosum* can occur in the absence of a differentiated mechanical layer.

Anther wall development in SHB cultivars of *V. corymbosum* ('Emerald' and 'Snowchaser') broadly follows the basic model proposed by Davis [38], in which the outer and inner secondary parietal layers arise from periclinal divisions of the primary parietal layer. Our

observations confirm that both derivatives undergo further periclinal divisions, resulting in a transient multilayered structure during early ontogeny. While the outer derivative does not form a typical fibrous endothecium, it produces a persistent subepidermal stratum analogous to the so-called "endothecial" layer described in other Ericaceae [7]. Although early floral primordia were not available for analysis, we infer that the anther epidermis derives from the L1 layer of the floral meristem, while the wall layers originate from L2, and the connective tissue from L3. This interpretation is consistent with the general pattern described for dicot flowers, in which the L1 and L2 layers contribute to the formation of the anther lobes, whereas L3 gives rise to internal vasculature and connective tissue [39–42].

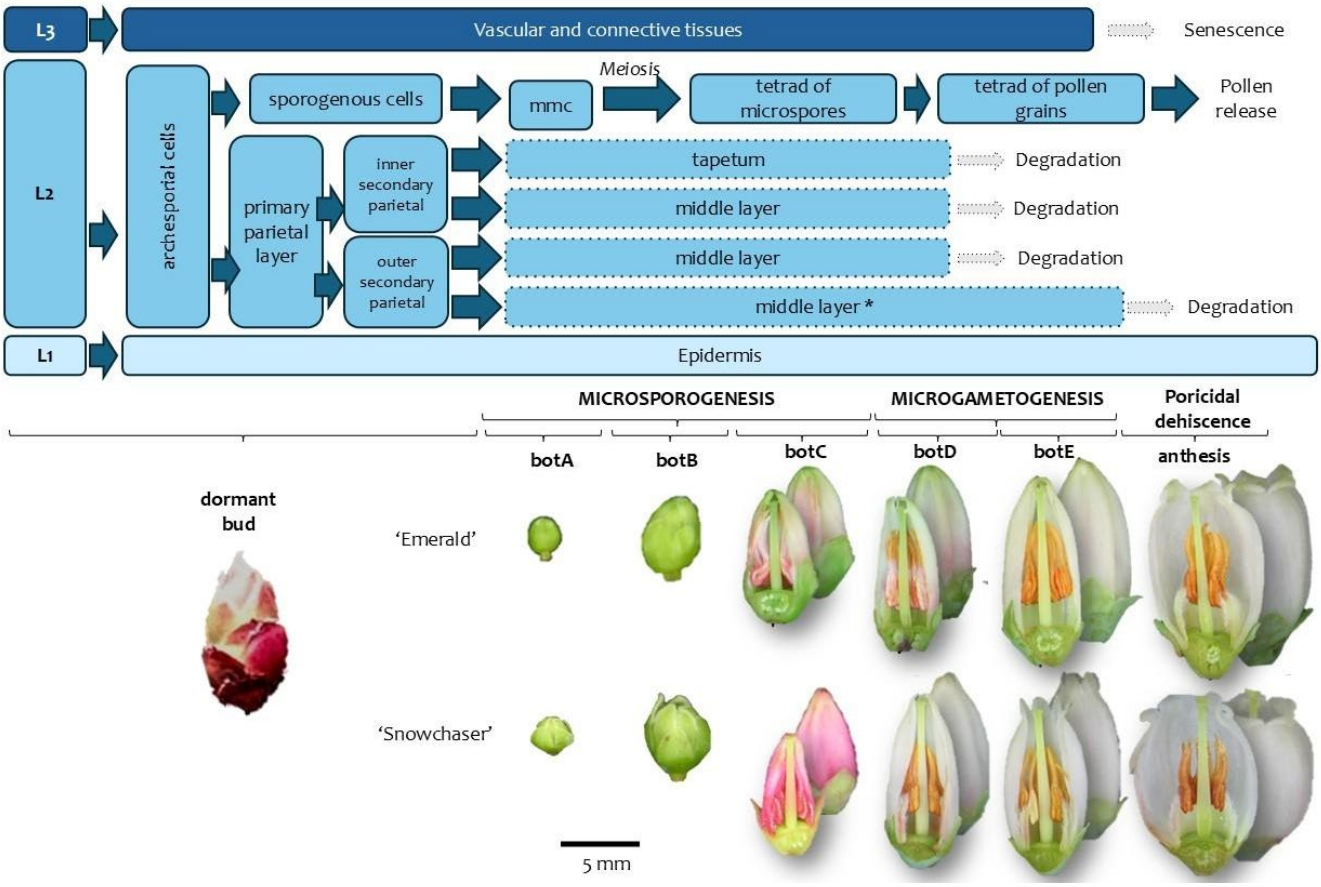


Figure 7. Summary diagram of anther development in *V. corymbosum*, illustrating the sequence of wall layer formation and their progressive degradation during pollen development. The epidermis remains as the only persistent layer at anthesis. Representative floral stages (db to ant) are shown below as longitudinal sections of 'Emerald' and 'Snowchaser', included to illustrate the corresponding morphological stages and confirm their developmental equivalence. Abbreviations: botA–E, floral buds A to E stages; L1–L3, histogenic layers of the floral meristem; ml *, middle layer corresponding to the hypodermal "endothecial" layer proposed by Hermann and Palser [7]; mmc, microspore mother cells.

Based on these findings, we propose a distinct pattern of anther wall formation, designated here as the Ericaceous type (Figure 8). In both cultivars, a single subepidermal layer remains throughout development, but we interpret it as a middle layer rather than an endothecium, given the consistent absence of secondary wall thickenings, key features of endothecial identity and dehiscence function in most angiosperms. This layer shows no signs of lignification and lacks structural traits typically associated with mechanical support. Its position and histological behavior are instead consistent with transient middle

layers, which often collapse during microsporogenesis. As a result, the mature anther wall in both cultivars consists solely of the epidermis, with no functional endothecium.

This distinctive pattern, characterized by the absence of a functional endothecium and the persistence of a non-lignified subepidermal layer, may represent a conserved trait within Ericaceae. As such, the Ericaceous type of anther wall formation proposed here not only contributes to the understanding of reproductive anatomy in *V. corymbosum*, but may also serve as a diagnostic feature of phylogenetic and functional relevance within the family.

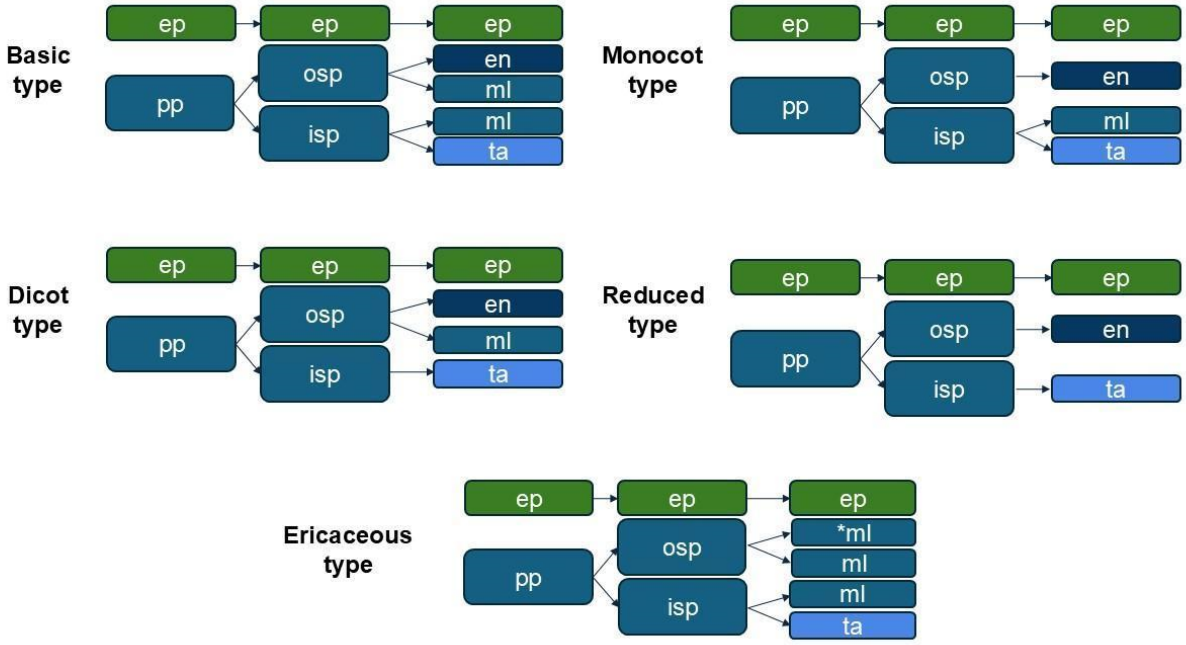


Figure 8. Comparative anther wall development patterns in Angiosperms, including the proposed Ericaceous type based on the classification by Davis [38] as adapted by Åstrand et al. [43]. All types derive from a primary parietal stratum giving rise to outer and inner secondary parietal layers. The Ericaceous type is characterized by the absence of a differentiated endothecium and the persistence of a subepidermal layer interpreted as a middle layer (* ml). Abbreviations: en, endothecium; ep, epidermis; isp, inner secondary parietal stratum; ml, middle layer; osp, outer secondary parietal stratum; pp, primary parietal stratum; ta, tapetum.

4.1.2. Microsporogenesis and Pollen Development

In Ericaceae, microsporogenesis typically involves meiotic divisions with simultaneous cytokinesis, leading to the formation of tetrahedral or occasionally decussate tetrads, with callose walls deposited after the second meiotic division [7,33]. However, an exception to this pattern has been documented in *Enkianthus* (Ericaceae), where the microspores separate after meiosis and are released as individual pollen grains [7].

Microsporogenesis in *V. corymbosum* NHB has been previously described for the cultivars 'Bluecrop' and 'Croatan', where archesporial cells give rise to both tapetal cells and microspore mother cells (MMCs), which undergo simultaneous cytokinesis after meiosis to form persistent tetrads [17,18]. In contrast, studies on *V. nummularia*, *V. serratum*, and *V. retusum* reported direct formation of MMCs from sporogenous tissue, without a distinct archesporial stage [33].

Subsequently, microgametogenesis proceeds according to the conventional pattern observed in Ericaceae: each microspore undergoes mitosis to produce a large vegetative cell enclosing a smaller generative cell, which migrates toward the center of the pollen grain and localizes near the vacuole [7]. By the time of anthesis and tetrad release, pollen

grains are bicellular [7,33]. In our study, CLSM analyses confirmed the presence of two distinct nuclei within mature pollen grains, consistent with this developmental stage. These findings confirm that pollen development in *V. corymbosum* cultivars 'Emerald' and 'Snowchaser' follows the conserved ontogenetic patterns described for other Ericaceae, both in the formation of persistent tetrads and in the bicellular nature of mature pollen grains.

In parallel with microspore and pollen development, the behavior of the tapetum was also examined, given its critical role during microsporogenesis. The tapetum in *V. nummularia*, *V. serratum*, and *V. retusum* is of the secretory type and becomes binucleate during meiotic prophase [33]. A similar secretory tapetum was observed in *V. corymbosum* cv. 'Sharpblue', well developed at early meiotic stages and it begins to degenerate at the tetrad stage [44]. Our histological observations in 'Emerald' and 'Snowchaser' confirm this pattern: the tapetum exhibits secretory characteristics and initiates degeneration during the tetrad stage. These findings are consistent with those reported for other *Vaccinium* species and support a conserved tapetal developmental pattern within the genus.

Overall, the developmental sequence observed in *V. corymbosum* SHB reflects the conserved reproductive strategy of Ericaceae.

4.1.3. Tubule Development and Persistent Pollen Tetrads Release

In Ericaceae, anthers terminate apically in long sterile extensions known as tubules (also called "awns" or "tubes"), which are initially solid but become hollow at maturity, allowing pollen release through apical pores [34]. Tubules are present in *V. corymbosum* and several related species, including *V. albicans*, *V. stamineum*, *V. myrtilloides*, *V. vitis-idaea*, and *V. meridionale* Swartz [7,34,35,45,46]. In *Vaccinium* species, it is common for the thecae of each anther lobe to fuse apically and extend into these tubules, leading Stephens et al. [35] to consider the anthers functionally bilocular. This structural arrangement plays a key role in the poricidal dehiscence mechanism characteristic of the group.

The anatomical configuration of the tubules directly influences the mode of dehiscence, which in Ericaceae is typically poricidal, occurring through circular, elliptical, or oblique pores at the apex of the tubules, and only rarely through longitudinal openings [7,47]. According to Kriebel et al. [8], this poricidal pattern is consistent within Vaccinioideae, a finding confirmed by the present observations. The formation of apical pores is associated with the breakdown of preformed tissues in the anther wall [36]. In *V. albicans*, tubules become hollow at the tetrad stage through a combination of tissue collapse and resorption, while in *V. stamineum*, hollowing results from collapse alone [46]. In 'Emerald' and 'Snowchaser', we observed that tissue breakdown initiates at the apex of the tubule and progresses basally and centrifugally. This pattern is consistent with earlier descriptions in *Vaccinium*, where degradation begins at the internal surface at the site of pore formation [31].

In addition to tubule orientation, stamen inversion was evaluated as a potential factor influencing pollen release. Stamen inversion, a phenomenon documented in Ericaceae, involves a shift from extrorse to introrse stamens and varies across subfamilies. It is typical of early-inversion clades such as Ericoideae Link, Styphelioideae Sweet, and Vaccinioideae [7,31,32,48]. Although Hermann and Palser [7] reported inversion in most of the species they examined, their study did not include *V. corymbosum*. In all observations of 'Emerald' and 'Snowchaser', the tubules were consistently oriented toward the stigma, ruling out stamen inversion throughout development up to and including dehiscence. The absence of inversion in the present study suggests that, if it occurs in *V. corymbosum*, it may take place at earlier developmental stages.

In terms of pollen dispersal, a consistent trait within Vaccinioideae is the release of permanent tetrads, reported in numerous species including *V. corymbosum* [7,35,49]. The

cultivars analyzed in this study also exhibited pollen release in tetrads, reinforcing this pattern within the subfamily.

These observations highlight the structural and functional integration of anther components in *V. corymbosum* SHB, contributing to a specialized and efficient pollen release mechanism adapted to buzz pollination.

4.2. Floral Staging and Its Correlation with Androecium Development

To support the anatomical analysis of androecium development, we proposed a floral staging system based on measurable external traits such as bud size, corolla visibility, and anther coloration (Table 2). This scale effectively distinguished key developmental stages from dormant bud to anthesis and proved consistent across both cultivars, despite slight differences in floral dimensions. This staging framework provided a reliable basis for correlating external morphology with internal developmental processes.

Each floral stage corresponded closely with specific histological events related to androecium development, particularly during microsporogenesis and microgametogenesis. These included critical transitions such as meiosis, tetrad formation, tapetum degradation, the appearance of bicellular pollen grains, and the onset of anther dehiscence. This correlation between external morphology and internal developmental status enables the precise identification of key timepoints for cytological sampling and controlled pollination.

Beyond its anatomical relevance, the proposed staging system also offers practical advantages over broader phenological frameworks such as the Michigan State University [19] and BBCH scales [20], which provide useful plant-level descriptors. By focusing on flower-level traits, our staging system enhances developmental resolution and offers practical value for reproductive, anatomical, and breeding studies. In particular, it may facilitate the accurate selection of floral material for targeted crosses or histological analyses, supporting breeding programs in low-chill environments where fine-scale phenological control is critical.

5. Conclusions

The results of this study highlight the structural consistency of the androecium in *V. corymbosum* SHB, revealing conserved features such as trichome presence, papillae distribution, and stamen wall organization across cultivars. The minor variation in vascular bundle termination and trichome abundance suggests potential intra-specific diversity, but overall, the floral androecium architecture in 'Emerald' and 'Snowchaser' conforms to the patterns previously described for other *Vaccinium* species and Ericaceae members.

The most conserved stamen features within Ericaceae include the presence of a binucleate glandular tapetum, the absence of fibrous endothecium, simultaneous cytokinesis resulting in tetrahedral tetrads, and the release of binucleate tricolporate pollen grains as tetrads. The results obtained confirm the presence of these traits in the 'Emerald' and 'Snowchaser' cultivars of *V. corymbosum* SHB, providing further evidence for the stability of these characters within the subfamily Vaccinioideae.

Based on histological and developmental data, we propose a distinct pattern of anther wall formation: the Ericaceous type, characterized by the transient presence of a subepidermal layer with the morphology and behavior of a middle layer, and by the absence of endothecial thickenings. At anthesis, the anther wall is reduced to the epidermis only. This pattern may serve as a diagnostic trait of phylogenetic and functional relevance within the family.

In addition, the staging framework established here complements existing systems (MSU, BBCH), offering a refined tool for developmental studies in SHB.

Understanding the basic aspects of a species' reproductive biology, particularly under specific environmental conditions, provides a theoretical foundation for the development of breeding programs based on controlled crosses. In this context, the findings of this study may support the advancement of breeding initiatives in non-traditional blueberry-growing regions.

Author Contributions: Investigation, Formal analysis, Writing—original draft, Writing—review & editing, Visualization: J.M.R. & A.M.G.; Conceptualization: A.M.G., P.A.L. & M.F.G.; Supervision, Writing—review & editing, Funding acquisition: P.A.L., A.M.G. & M.F.G. All authors have read and agreed to the published version of the manuscript.

Funding: This research was funded by the Universidad Nacional del Nordeste, grant numbers SGCyT-PI 20P001 (to AMG) and SGCyT-PI 22P002 (to PAL); and by Instituto Nacional de Tecnología Agropecuaria, grant number 2023-PE-L01-I105 (to MFG).

Data Availability Statement: The authors confirm that the data supporting the findings of this study are available within the article.

Acknowledgments: We thank the establishments "Fruitcrop S.A. Quinta Palma Sola" and "Blueberries S.A." (Concordia, Entre Ríos), as well as "El Panqueque S.R.L." (Bella Vista, Corrientes), for kindly granting access to their blueberry fields for sample collection.

Conflicts of Interest: The authors declare no conflicts of interest.

Abbreviations

The following abbreviations are used in this manuscript:

ac	Archesporial cells
acl	Apical cleft
an	Anther
ant	Flower at anthesis
ap	Apical pore
ca	Calyx
CLSM	Confocal laser scanning microscopy
co	Corolla
col	Colporus
ct	Connective tissue
db	Dormant bud
dr	Dorsal reinforcement
ep	Epidermis
en	Endothecium
fi	Filament
gyn	Gynoecium
isp	Inner secondary parietal layer
L1–L3	Histogenic layers of the floral meristem
LM	Light microscopy
lo	Locule
LS	Longitudinal section
ml	Middle layers
mmc/MMC	Microspore mother cell
MSU	Michigan State University
n	Nectary
NHB	Northern highbush blueberries
nm	Nectarostome
nt	Tapetal cell nucleus

osp	Outer secondary parietal layer
ov	Ovary
pa	Papilla
pc	Parenchymatous cells
pn	Pollen nuclei
pp	Primary parietal layer/stratum
ps	Pollen sac
s	Sporogenous cell
SEM	Scanning electron microscopy
sg	Stigma
SHB	Southern highbush blueberries
SM	Stereomicroscopy
st	Style
ta	Tapetum
tet	Tetrad of microspores
th	Theca
tpg	Tetrad of pollen grains
tr	Trichome
TS	Transversal section
tu	Tubule
vb	Vascular bundle

References

1. Brazelton, C.; Fain, C.; Ogg, M.; Riquelme, C.; Rodriguez, V.; Ilyas, S. *Global State of the Blueberry Industry Report 2024*; International Blueberry Organization: El Dorado Hills, CA, USA, 2024; pp. 1–239.
2. Edger, P.P.; Iorizzo, M.; Bassil, N.V.; Benevenuto, J.; Ferrão, L.F.V.; Giongo, L.; Hummer, K.; Lawas, L.M.F.; Leisner, C.P.; Li, C.; et al. There and Back Again; Historical Perspective and Future Directions for Vaccinium Breeding and Research Studies. *Hortic. Res.* **2022**, *9*, uhac083. [CrossRef]
3. Retamales, J.B.; Hancock, J.F. *Blueberries*; CABI: Wallingford, UK, 2018; ISBN 9781780647265.
4. Lobos, G.A.; Hancock, J.F. Breeding Blueberries for a Changing Global Environment: A Review. *Front. Plant Sci.* **2015**, *6*, 782. [CrossRef]
5. Rivadeneira, M.F. Variedades de Arándanos Disponibles en Argentina. Available online: https://www.aianer.com.ar/web/download/202010inta_concordia_variedades_de_arandanos.pdf (accessed on 10 September 2025).
6. Cromie, J.; Ternest, J.J.; Komatz, A.P.; Adunola, P.M.; Azevedo, C.; Mallinger, R.E.; Muñoz, P.R. Genotypic Variation in Blueberry Flower Morphology and Nectar Reward Content Affects Pollinator Attraction in a Diverse Breeding Population. *BMC Plant Biol.* **2024**, *24*, 814. [CrossRef]
7. Hermann, P.M.; Palser, B.F. Stamen Development in the Ericaceae. I. Anther Wall, Microsporogenesis, Inversion, and Appendages. *Am. J. Bot.* **2000**, *87*, 934–957. [CrossRef]
8. Kriebel, R.; Rose, J.P.; Bastide, P.; Jolles, D.; Reginato, M.; Sytsma, K.J. The Evolution of Ericaceae Flowers and their Pollination Syndromes at a Global Scale. *Am. J. Bot.* **2023**, *110*, e16220. [CrossRef] [PubMed]
9. Ehlenfeldt, M.K.; Polashock, J.J. Highly Fertile Intersectional Blueberry Hybrids of *Vaccinium padifolium* Section Hemimyrtillus and V. Corymbosum Section Cyanococcus. *J. Am. Soc. Hort. Sci.* **2014**, *139*, 30–38. [CrossRef]
10. Ehlenfeldt, M.K.; Luteyn, J.L. Fertile Intersectional F1 Hybrids of 4x *Vaccinium meridionale* (Section Pyxothamnus) and Highbush Blueberry, V. corymbosum (Section Cyanococcus). *HortScience* **2021**, *56*, 318–323. [CrossRef]
11. Chu, Y.; Lyrene, P.M. Artificial Induction of Polyploidy in Blueberry Breeding: A Review. *HortScience* **2025**, *60*, 100–110. [CrossRef]
12. De Storme, N.; Geelen, D. Sexual Polyploidization in Plants—Cytological Mechanisms and Molecular Regulation. *New Phytol.* **2013**, *198*, 670–684. [CrossRef] [PubMed]
13. Drummond, F. Reproductive Biology of Wild Blueberry (*Vaccinium angustifolium* Aiton). *Agriculture* **2019**, *9*, 69. [CrossRef]
14. Quiroga-Arcila, A.M.; McCune, F.; Fournier, V.; Giovenazzo, P. Bee-Ing a Pollinator: Constraints, Concerns, and Challenges of Lowbush Blueberry Pollination. *Int. J. Fruit Sci.* **2025**, *25*, 28–63. [CrossRef]
15. Bieniasz, M.E.; Konieczny, A.M. Opportunities to Improve Effectiveness of Pollination of Blueberry CV. 'Bluecrop'. *Agriculture* **2022**, *12*, 2126. [CrossRef]

16. Leposavić, A.; Glišić, I.; Đorđević, M.; Jevremović, D.; Zejak, D.; Cerović, R. The Effect of Pollination Variant and Temperature on Reproductive Behaviour of Some Highbush Blueberry (*Vaccinium corimbosum* L.) Cultivars. *Appl. Fruit Sci.* **2024**, *66*, 2077–2089. [CrossRef]
17. Bieniasz, M. The Differentiation of Highbush Blueberry Flower Buds. *Acta Hortic.* **2012**, *932*, 117–122. [CrossRef]
18. Gough, R.E.; Shutak, V.G.; Hauke, R.L. Growth and Development of Highbush Blueberry II. Reproductive Growth, Histological Studies. *J. Am. Soc. Hortic. Sci.* **1978**, *103*, 476–479. [CrossRef]
19. Michigan State University. Growth Stages—Blueberries. Available online: https://www.canr.msu.edu/blueberries/growing_blueberries/growth-stages (accessed on 15 June 2025).
20. Wichura, M.A.; Koschnick, F.; Jung, J.; Bauer, S.; Wichura, A. Phenological Growth Stages of Highbush Blueberries (*Vaccinium* Spp.): Codification and Description According to the BBCH Scale. *Botany* **2024**, *102*, 428–437. [CrossRef]
21. Ramos, S.; De Ruyver, R.; Gattinoni, N.; Garin, R.; Garrán, S. *Estación Agrometeorológica del INTA Concordia. 50 Años de Servicio a la Comunidad*; INTA: Ciudad de Buenos Aires, Argentina, 2018; pp. 1–53.
22. Tasi, H.A.; Bedendo, D.J.; Pausich, G.M.; López, L.O.; Schulz, G.; Garran, S.M.; Garin, O.R. *Carta de Suelos de La Estación Experimental Agropecuaria Concordia. Departamento Concordia, Provincia de Entre Ríos. Escala 1:5000*; INTA: Ciudad de Buenos Aires, Argentina, 2011; pp. 1–107.
23. Maidana, M.M.; Contreras, F.I.; Vasek, O.M. La Variabilidad Climática como condicionante de presencia de Bacterias Lácticas Autóctonas, Noroeste de La Provincia de Corrientes. Argentina. *Geográfica Digit.* **2021**, *17*, 81. [CrossRef]
24. Schindelin, J.; Arganda-Carreras, I.; Frise, E.; Kaynig, V.; Longair, M.; Pietzsch, T.; Preibisch, S.; Rueden, C.; Saalfeld, S.; Schmid, B.; et al. Fiji: An Open-Source Platform for Biological-Image Analysis. *Nat. Methods* **2012**, *9*, 676–682. [CrossRef]
25. Gonzalez, A.M. ImageJ: Una herramienta indispensable para medir el mundo Biológico. *Folium* **2018**, *1*, 1–17.
26. González, A.M.; Cristóbal, C.L. Anatomía y Ontogenia de Semillas de Helicteres lhotzkyana (Sterculiaceae). *Bonplandia* **1997**, *9*, 287–294. [CrossRef]
27. Johansen, D.A. *Plant Microtechnique*; McGraw-Hill Book Company, Incorporated: New York, NY, USA, 1940; ISBN 0070325405.
28. Luque, R.; Sousa, H.C.d.; Kraus, J.E. Métodos de Coloração de Roeser (1972): Modificado—E Kropp (1972) Visando a substituição do Azul de Astra Por Azul de Alcião 8GS Ou 8GX. *Acta Bot. Bras.* **1996**, *10*, 199–212. [CrossRef]
29. Vasco, A.; Thadeo, M.; Conover, M.; Daly, D.C. Preparation of Samples for Leaf Architecture Studies, a Method for Mounting Cleared Leaves. *Appl. Plant Sci.* **2014**, *2*, apps.1400038. [CrossRef] [PubMed]
30. Almeida, P.M.; Carvalho, C.R. NOR-Associated Heterochromatin of Pepper Chromosomes Stained with Acridine Orange. *Caryologia* **2004**, *57*, 172–176. [CrossRef]
31. Matthews, J.R.; Knox, E.M. The Comparative Morphology of the stamen in the Ericaceae. *Trans. Bot. Soc. Edinb.* **1927**, *29*, 243–281. [CrossRef]
32. Stevens, P.F. A Classification of the Ericaceae: Subfamilies and Tribes. *Bot. J. Linn. Soc.* **1971**, *64*, 1–53. [CrossRef]
33. Venkateswarlu, J.; Maheswari Devi, H. An Embryological Approach to the Taxonomic Status of Vacciniaceae. *Proc. Indian Acad. Sci.* **1973**, *78*, 282–291. [CrossRef]
34. Palser, B.F. Studies of Floral Morphology in the Ericales. V. Organography and Vascular Anatomy in Several United States Species of the Vacciniaceae. *Bot. Gaz.* **1961**, *123*, 79–111. [CrossRef]
35. Stephens, D.T.; Levesque, D.E.; Davis, A.R. Pollen-Ovule Ratios in Seven Species of Vaccinium (Ericaceae) and Stamen Structure in *Vaccinium myrtilloides* and *Vaccinium vitis-idaea*. *Botany* **2012**, *90*, 599–614. [CrossRef]
36. Artopoeus, V.A. Über Den Bau Und Die Öffnungsweise der antheren und die entwickelung der samen der Erikaceen. *Flora Oder Allg. Bot. Ztg.* **1903**, *92*, 309–345.
37. D'arcy, W.G.; Keating, R.C.; Buchmann, S.L. The Calcium Oxalate Package or So-Called Resorption Tissue in Some Angiosperm Anthers. In *The Anther: Form, Function and Phylogeny*; Cambridge University Press: Cambridge, UK, 1996; pp. 159–191, ISBN 9780521480635.
38. Davis, G.L. *Systematic Embryology of the Angiosperms*; John Wiley & Sons: New York, NY, USA, 1966; ISBN 9780471198871.
39. Xue, J.-S.; Yao, C.; Xu, Q.-L.; Sui, C.-X.; Jia, X.-L.; Hu, W.-J.; Lv, Y.-L.; Feng, Y.-F.; Peng, Y.-J.; Shen, S.-Y.; et al. Development of the Middle Layer in the Anther of Arabidopsis. *Front. Plant Sci.* **2021**, *12*, 634114. [CrossRef]
40. Biswas, R.; Chaudhuri, S. The Tale of Tapetum: From Anther Walls to Pollen Wall. *Nucleus* **2024**, *67*, 611–630. [CrossRef]
41. Goldberg, R.B.; Beals, T.P.; Sanders, P.M. Anther Development: Basic Principles and Practical Applications. *Plant Cell* **1993**, *5*, 1217–1229. [CrossRef]
42. Scott, R.J.; Spielman, M.; Dickinson, H.G. Stamen Structure and Function. *Plant Cell Online* **2004**, *16*, S46–S60. [CrossRef]
43. Åstrand, J.; Knight, C.; Robson, J.; Talle, B.; Wilson, Z.A. Evolution and Diversity of the Angiosperm Anther: Trends in Function and Development. *Plant Reprod.* **2021**, *34*, 307–319. [CrossRef]
44. Huang, Y.H.; Johnson, C.E.; Sundberg, M.D. Floral Morphology and Development of 'Sharpblue' Southern Highbush Blueberry in Louisiana. *J. Am. Soc. Hortic. Sci.* **1997**, *122*, 630–633. [CrossRef]

45. Chamorro, F.J.; Nates-Parra, G. Floral and Reproductive Biology of *Vaccinium meridionale* (Ericaceae) in the Eastern Andes of Colombia. *Rev. Biol. Trop.* **2015**, *63*, 1197–1212. [CrossRef]
46. Hermann, P.M.; Palser, B.F. Stamen Development in the Ericaceae. II. Granular Pouches and Dehiscence. *Flora Morphol. Distrib. Funct. Ecol. Plants* **2018**, *239*, 122–140. [CrossRef]
47. Matthews, J.R.; Taylor, G. The Structure and development of the Stamen in *Erica hirtiflora*. *Trans. Bot. Soc. Edinb.* **1927**, *29*, 235–242. [CrossRef]
48. Kron, K.A.; Judd, W.S.; Stevens, P.F.; Crayn, D.M.; Anderberg, A.A.; Gadek, P.A.; Quinn, C.J.; Luteyn, J.L. Phylogenetic Classification of Ericaceae: Molecular and Morphological Evidence. *Bot. Rev.* **2002**, *68*, 335–423. [CrossRef]
49. Golam Sarwar, A.K.M.; Ito, T.; Takahashi, H. An Overview of Pollen Morphology and its Relevance to the Sectional Classification of *Vaccinium* L. (Ericaceae). *Jpn. J. Palynol.* **2006**, *52*, 15–34.

Disclaimer/Publisher's Note: The statements, opinions and data contained in all publications are solely those of the individual author(s) and contributor(s) and not of MDPI and/or the editor(s). MDPI and/or the editor(s) disclaim responsibility for any injury to people or property resulting from any ideas, methods, instructions or products referred to in the content.